Articles

Structure–Activity Relationship of *S*-Trityl-L-Cysteine Analogues as Inhibitors of the Human Mitotic Kinesin Eg5

Salvatore DeBonis,[†] Dimitrios A. Skoufias,[‡] Rose-Laure Indorato,[‡] François Liger,[§] Bernard Marquet,[§] Christian Laggner,[||] Benoît Joseph,[§] and Frank Kozielski*[,⊥]

Laboratoire des Moteurs Moléculaires and Laboratoire des Protéines du Cytosquelette, Institut de Biologie Structurale, 41, rue Jules Horowitz, 38027 Grenoble Cedex 01, France, Chimiothèque de l'UMR - CNRS 5246, Université de Lyon, Université Claude Bernard Lyon 1, 43, Boulevard du 11 Novembre 1918, 69622 Villeurbanne, France, Department of Pharmaceutical Chemistry, Institute of Pharmacy and Center for Molecular Biosciences (CMBI), University of Innsbruck, Innrain 52c, 6020 Innsbruck, Austria, and The Beatson Institute for Cancer Research, Molecular Motors Laboratory, Garscube Estate, Switchback Road, Bearsden, Glasgow G61 1BD, United Kingdom

Received May 25, 2007

The human kinesin Eg5 is a potential drug target for cancer chemotherapy. Eg5 specific inhibitors cause cells to block in mitosis with a characteristic monoastral spindle phenotype. Prolonged metaphase block eventually leads to apoptotic cell death. *S*-trityl-L-cysteine (STLC) is a tight-binding inhibitor of Eg5 that prevents mitotic progression. It has proven antitumor activity as shown in the NCI 60 tumor cell line screen. It is of considerable interest to define the minimum chemical structure that is essential for Eg5 inhibition and to develop more potent STLC analogues. An initial structure–activity relationship study on a series of STLC analogues reveals the minimal skeleton necessary for Eg5 inhibition as well as indications of how to obtain more potent analogues. The most effective compounds investigated with substitutions at the *para*-position of one phenyl ring have an estimated K_i^{app} of 100 nM *in vitro* and induce mitotic arrest with an EC_{50} of 200 nM.

Introduction

The function of most motor proteins of the kinesin superfamily is related to intracellular transport, such as organelles and vesicles. A smaller group of kinesins however is implicated at different discrete steps of the cell division cycle.[1] Some of these mitotic kinesins are potential drug targets for the development of small molecules inhibiting cell proliferation and thus tumor growth.[2–4] The most prominent mitotic kinesin is HsEg5 (or KSP[a]), which is involved in the formation of the bipolar spindle.[5] The duplicated centrosomes of cells incubated with these inhibitors fail to separate due to the inhibition of Eg5, and microtubules (MTs) emanate from a center formed by the four centrioles, surrounded by a ring of chromosomes. Cells remain in mitotic arrest and eventually escape abnormally, leading to apoptosis. This phenotype is easy to distinguish from normal bipolar cells. Several inhibitors have been discovered that arrest cells in mitosis by targeting Eg5[6–10] and now serve as a starting point for the development of more potent inhibitors[11,12] or already represent chemically optimized inhibitors (Figure 1).[13,14] The most advanced Eg5 inhibitor is "Ispinesib", an enantiomeric pure quinazolinone derivative obtained after chemical optimization (clinical phase II trials). A related compound, CK0106023, inhibits the basal Eg5 ATPase activity with a K_i of 12 nM and inhibits tumor growth tested on 12 different tumor cell lines with a GI_{50} of about 364 nM.[10]

Using an in vitro screening procedure, we recently identified a series of new Eg5 inhibitors inducing mitotic arrest in HeLa cells.[9] The most potent of these inhibitors was *S*-trityl-L-cysteine (STLC). Although known for some time to induce mitotic arrest,[15] the protein target had remained unknown. STLC inhibits basal ($K_i^{app} \sim 26$ nM) as well as MT-activated Eg5 ATPase activity ($IC_{50} = 140$ nM) and MT gliding in motility assays ($IC_{50} = 0.5$ μM). In cell-based assays, STLC induces mitotic arrest in HeLa cells ($IC_{50} = 0.7$ μM)[16] and subsequently apoptosis,[17] relating to its tumor growth inhibition activity ($GI_{50} = 1.31$ μM), as shown in the NCI 60 tumor cell line screen (http://dtp.nci.nih.gov). STLC is a reversible inhibitor that does not compete with either ATP or MTs, and the STLC binding site on Eg5 has been narrowed down to a region forming an induced-fit pocket about 12 Å away from the active nucleotide-binding pocket,[18] similar to that of monastrol. However, detailed structural data on the complex between STLC and Eg5 are not yet available.

Here we have undertaken an initial structure–activity relationship study using 64 STLC analogues. Based on the molecules available for this study, we were able to describe a minimal skeleton for inhibition of Eg5. We also identified several STLC analogues that are more potent in inducing mitotic arrest in cell-based assays than the original compound. Furthermore, selected analogues were docked into available X-ray crystal structures

* To whom correspondence should be addressed. Tel.: +44-141-330-3186. Fax: +44-141-942-6521. E-mail: f.kozielski@beatson.gla.ac.uk.

[†] Laboratoire des Moteurs Moléculaires.

[‡] Laboratoire des Protéines du Cytosquelette.

[§] Université de Lyon.

[||] University of Innsbruck.

[⊥] The Beatson Institute for Cancer Research.

[a] Abbreviations: DMSO, dimethylsulfoxide; EC_{50}, half-maximum effective inhibitory concentration; FITC, fluorescein isothiocyanate; GI_{50}, half-maximum growth inhibitory concentration; IC_{50}, median inhibitory concentration; K_i^{app}, apparent inhibitor constant; KSP, kinesin spindle protein; MTs, microtubules; MPM2, mitotic protein monoclonal 2; NCI, National Cancer Institute; n.d., not determined; n.i., no inhibition; OTLS, *O*-trityl-L-serine; PBS, phosphate buffer saline; PDB, protein data bank; PE, petroleum ether; STDC, *S*-trityl-D-cysteine; STLC, *S*-trityl-L-cysteine; TLC, thin layer chromatography; TMS, tetramethylsilane.

10.1021/jm070606z CCC: $40.75
Published on Web 02/12/2008

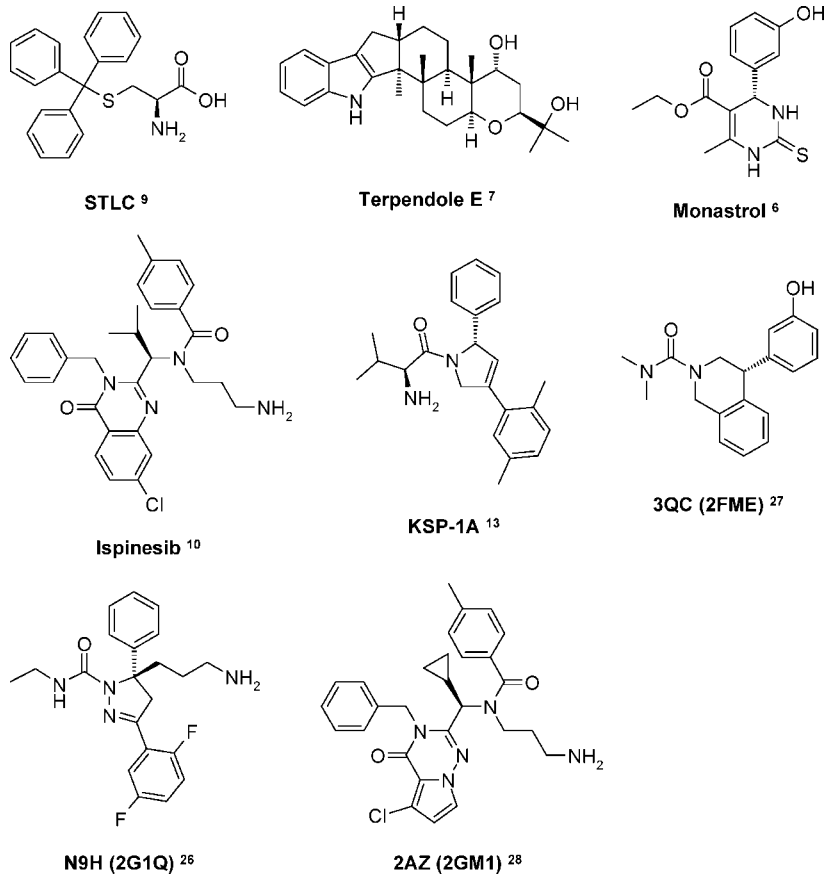

Figure 1. Representative overview of known Eg5 inhibitors, including the ligands of the PDB complexes that were used for our docking studies with both ligand three-letter and complex four-letter codes.

Scheme 1[a]

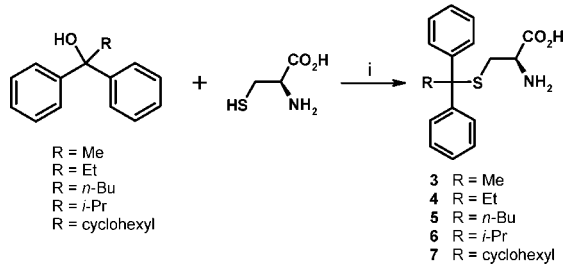

[a] Reagents and conditions: (i) $BF_3 \cdot Et_2O$, AcOH, rt, 2 h.

of Eg5. From this we deduced the possible binding mode of the reported compounds and to explain the SAR data obtained. This study is a first step toward a better understanding of inhibition of a motor protein by STLC and a starting point for the development of more potent analogues.

Chemistry. To determine the functional groups of STLC responsible for inhibition of Eg5, 64 STLC analogues were tested. These compounds were either obtained from the NCI database (compounds **1**, **2**, **8**–**31**, and **35**–**65**) or synthesized in the laboratory (compounds **3**–**7** and **32**−**34**). Condensation of diphenylalkylalcohols $Ph_2C(R)OH$ (R = Me, Et, *n*-Bu, *i*-Pr, and cyclohexyl)[19,20] with L-cysteine in the presence of $BF_3 \cdot Et_2O$ afforded derivatives **3**–**7** in 25–69% yield (Scheme 1).[21] Compounds **32** and **33** were prepared in one- or two-step reactions following literature procedures (Scheme 2).[22] Nucleophilic substitution of bromopropylamine hydrobromide with tritylmercaptan in basic medium gave compound **32** in 82% yield. Similarly, the same reaction was performed in the presence of *N*-(4-bromobutyl)phthalimide and tritylmercaptan to give the phthalimido-*S*-trityl intermediate in 85% yield. The latter compound treated with hydrazine.hydrate at 50 °C led to the desired derivative **33** in 74% yield. Compound **34** was prepared by condensation of triphenylmethanol with L-serine in the presence of $BF_3 \cdot Et_2O$ (30% yield; Scheme 3).[23]

Biological Results and SAR Studies. Inhibition of Basal Eg5 ATPase Activity. The 64 different analogues were tested by first determining the IC_{50} value of the inhibition of basal Eg5 ATPase activity using inhibitor concentrations up to a maximum of 200 μM (Figure 2). The chemical structures of all compounds, the IC_{50} values for the inhibition of basal Eg5 ATPase activity and the EC_{50} values of mitotic arrest induced in HeLa cells are indicated in Tables 1−7 and Table 1 of the Supporting Information. Out of 65 compounds, 35 inhibited the basal Eg5 ATPase activity. These compounds were remeasured in triplicate under identical conditions (same Eg5 concentration, same buffers) to minimize the effect of tight-binding inhibitors, for which the IC_{50} value depends on the protein concentration used in the assay.[16] Activities for compounds **37**, **38**, **40**, **41**, and **52** have been just recently reported in a manuscript from a different group.[24]

Table 1 presents a first series of 10 compounds (including STLC as compound **1**, which serves as a control). In these compounds, the L-cysteine group remains unchanged and the central carbon atom of the non-natural amino acid side chain carries alkyl or aryl groups. The diphenyl compound **2** does not inhibit basal Eg5 activity. In contrast, diphenylalkyl derivatives with increasing linear (**3**–**5**) or branched (**6**–**7**) alkyl groups inhibit Eg5 activity. The α-napthyl derivative **8** was less potent than **1**, the β-napthyl derivative **9**, and the 3,4-methylenedioxyphenyl derivative **10**.

Scheme 2[a]

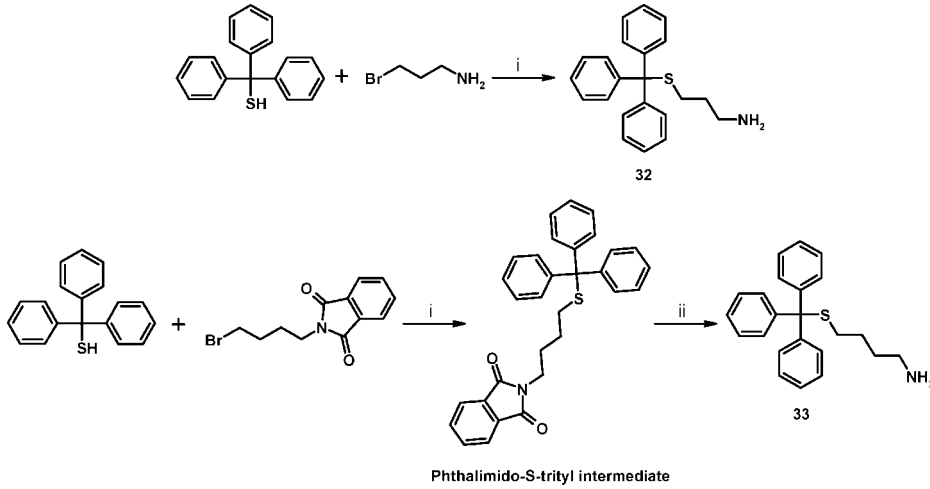

[a] Reagents and conditions: (i) NaH, DMF, rt, overnight; (ii) NH_2-NH_2·H_2O, EtOH/*n*-BuOH, 50 °C, 2 h.

Scheme 3[a]

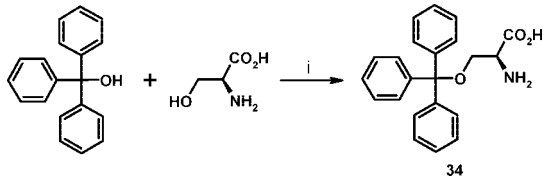

[a] Reagents and conditions: (i) BF_3·Et_2O, AcOH, rt, 2 h.

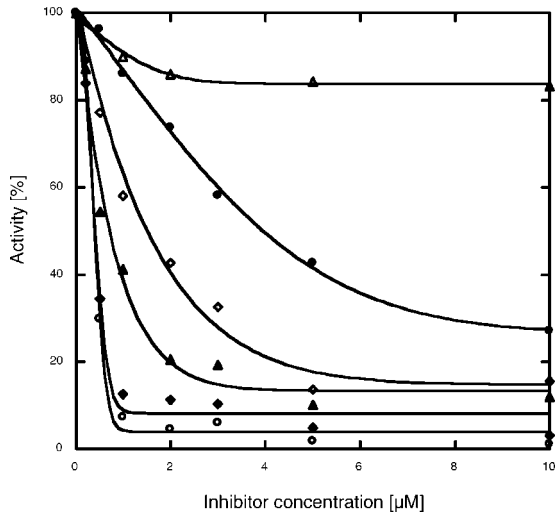

Figure 2. Dose–response plots showing the inhibition of basal Eg5 ATPase activity by a selected set of STLC analogues: **54** (open triangles), **45** (filled circles), **43** (open diamonds), **31** (filled triangles), **1** (filled diamonds), and **52** (open circles).

Table 2 presents nine compounds (**11**−**19**) containing the triphenylmethyl core structure with various atoms or groups attached to the methyl group. In these compounds, the sulfur atom, as present in STLC structure, is missing. Interestingly, none of these inhibits basal Eg5 activity, indicating the importance of certain elements of the cysteine group in the original STLC structure.

To investigate the importance of the L-cysteine group in more detail, we tested 15 compounds (**20**−**35**) with an unchanged triphenylmethyl core structure and different functional sulfur or oxygen groups, summarized in Table 3. Most of the tested compounds do not inhibit basal Eg5 ATPase activity. The minimum requirement for effective Eg5 inhibition is represented by compound **31**, which misses the carboxyl group of L-cysteine, but which inhibits basal Eg5 ATPase activity, with a K_i^{app} of 150 nM. Thus, the carboxyl group is not essential for Eg5 inhibition. Interestingly, compounds with one (**32**) or two (**33**) additional methyl groups do not significantly inhibit Eg5 activity, indicating that the chain length of the aminoalkyl group is also an important factor for proper inhibition. *O*-Trityl-L-serine (**34**, OTLS) is considerably less potent than STLC, with a K_i^{app} of 750 nM. In contrast, the amino group seems essential to retain the biological activity, since compound **35** (carboxyl group) does not inhibit basal Eg5 ATPase activity anymore.

To further confirm the importance of the primary amino group, we investigated five compounds with a modified amino group carrying different additional functional groups (Table 4). None of these compounds (**36**−**40**) inhibits basal Eg5 activity.

Table 5 contains STLC analogues (**41**−**47**), which carry modifications at the dispensable carboxy terminal group. The methyl ester group (derivative **41**) is almost as potent as STLC **1**. The introduction of steric hindrance with functional groups leads to compounds that are less active than STLC but still inhibit basal Eg5 ATPase activity, confirming that the carboxyl group is not essential for proper inhibition.

Table 6 contains compounds (**48**−**59**) that carry one, two, or three additional functional groups in the *para*-position at the three phenyl groups. The L-cysteinyl group remains unchanged. All compounds are inhibitors of basal Eg5 activity with K_i^{app} values ranging from 100 nM up to 35 μM.

Table 7 contains triphenyl compounds (**60**−**65**) that have an additional covalent bond connecting two phenyl substituents in the *ortho*-positions, thus leading to more rigid molecules that can no longer freely rotate around two of their three phenyl groups. Molecules from this group either inhibit basal Eg5 ATPase activity but with baselines between 30 and 60% or are no longer Eg5 inhibitors. Consequently, compound **60**, similar to STLC is considerably less active with a K_i^{app} of 1.5 μM. Compound **64**, containing an additional functional group at the amino substituent, is inactive (see Table 4). Compound **65** that contains two covalently interconnected phenyl groups and one naphthyl group would correspond to compound **8** (Table 1) and is less active (K_i^{app} = 0.9 μM, 60% baseline). Compounds (**61**–**63**) contain an additional methyl or halogene substituent in *para*-position of the freely rotationable phenyl group but are less effective or do not inhibit basal Eg5 activity at all, which

Table 1. Apparent K_i^{app} Values for the Inhibition of Basal Eg5 ATPase Activity and EC_{50} Values for Mitotic Arrest Determined Using Cell-Based Assays for Compounds **1–10**

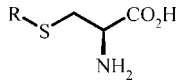

1-10

Compd	R	ATPase activity K_i^{app} [nM]	Cell-based assay EC_{50} [μM]
1	Tr	*50	0.7
2	-CH(Ph)$_2$	n.i.	> 5
3		2500	> 5
4		450	> 5
5	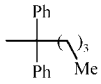	175	1.40
6	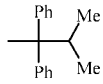	150	1.08
7	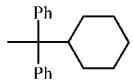	175	1.85
8	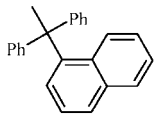	4000	> 5
9	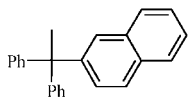	200	0.33
10	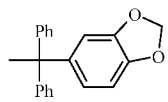	200	1.37

* Estimates of the K_i^{app} values can vary depending on the buffer and test conditions used.[16,35]

is in contrast to the results obtained for compounds **48**, **49**, **51**, where the same modification lead to compounds of similar activity. We conclude that, for effective Eg5 inhibition, the ability of the phenyl groups to assume different rotational angles is essential. Taken into account the set of analogues tested we conclude that the minimum requirement for effective Eg5 inhibition is represented by compound **31**.

To verify whether the new potent STLC analogues are tight-binding inhibitors of Eg5, like STLC,[16] we performed dose–response plots of fractional velocity as a function of STLC analogue concentration at four different Eg5 concentrations. Compounds **9**, **31**, **43**, and **50** were chosen because they belong to the most active compounds of their series. Like STLC (K_i^{app} of 50 nM, served as control), they are all tight-binding inhibitors with estimates of K_i^{app} values of 200 nM for **9**, 150 nM for **31**, 600 nM for **43**, and 250 nM for **50**, respectively (Figure 1, Supporting Information).

Table 2. IC_{50} Values for Inhibition of Basal Eg5 ATPase Activity for Compounds **11–19**

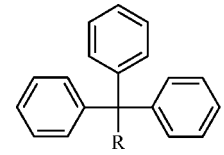

11-19

Compd	R	ATPase activity K_i^{app} [nM]
11	-Cl	n.i.
12	-Br	n.i.
13	-OH	n.i.
14	-OMe	n.i.
15	-NH$_2$	n.i.
16	-Me	n.i.
17	-Et	n.i.
18	-CH$_2$-C(OH)Me$_2$	n.i.
19	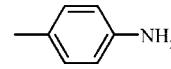	n.i.

Analogues that proved to be inhibitors of basal Eg5 ATPase activity were further tested using a phenotype cell-based assay by incubating HeLa cells with different analogues at a concentration of 5 μM. Inhibitors that induced less than 50% of mitotic cells displaying the monoastral spindle phenotype (Figure 3) were discarded and not investigated further (19 out of 35 compounds). To determine EC_{50} values for monoastral spindle formation for the remaining 16 molecules, dose–response plots were performed by incubating HeLa cells with increasing amounts of inhibitors (Figure 4). The analogues are ordered according to their potency to induce mitotic arrest in HeLa cells, and the results are summarized in Table 8. Nine analogues are less potent than STLC to arrest cells in mitosis, with EC_{50} values between 1.0 μM and 3.5 μM. Among them are the diphenylalkyl compounds that are potent Eg5 inhibitors in cell-based assays with IC_{50} values between 1.5 and 2 μM, indicating that three phenyl groups are more effective than two phenyl groups. Compound **31** lacks the carboxyl group present in STLC but is nearly as potent as STLC itself, confirming the previous finding that there is no stereoselectivity between STLC and STDC.[16] The other six analogues are more potent than STLC with EC_{50} values in cell-based assays reaching 200 nM. One characteristic feature of analogues that are more potent than STLC is that they all have additional functional groups in the *para*-position of one or two phenyl groups (compounds **49–52** and **57**) or that they have an additional cycle bridging the *meta*- and *para*-positions in one of the phenyl rings of the trityl group (**9**). Although compound **34** was active in in vitro-based assays with a K_i^{app} of 750 nM, it was ineffective in inducing monoastral spindles and in provoking mitotic arrest in cell-based assays at concentrations as high as 5 μM (data not shown).

Table 3. Apparent K_i^{app} Values for Inhibition of Basal Eg5 ATPase activity and for Mitotic Arrest in HeLa Cells for Compounds **20–35**

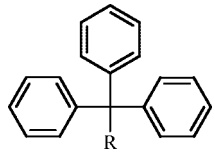

20-35

Compd	R	ATPase activity K_i^{app} [nM]	Cell-based assay EC_{50} [μM]
20	-SH	n.i.	n.d.
21	-S-CH_2-CH_3	n.i.	n.d.
22	-S-CH_2-Ph	n.i.	n.d.
23	-S-CO-Me	n.i.	n.d.
24	-S-CH_2-CH_2-Cl	n.i.	n.d.
25	-S-CH_2-CH_2-CO-Me	n.i.	n.d.
26	-S-CH_2-CH_2-OH	n.i.	n.d.
27	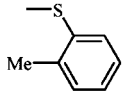	n.i.	n.d.
28	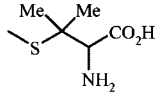	5230	> 5
29	-S-CH_2-CO_2Me	n.i.	n.d.
30	-S-CH_2-CH_2-CO_2Me	n.i.	n.d.
31	-S-CH_2-CH_2-NH_2	150	1.08
32	-S-CH_2-CH_2-CH_2-NH_2	n.i.	> 5
33	-S-CH_2-CH_2-CH_2-CH_2-NH_2	n.i.	> 5
34	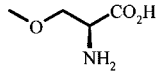	750	> 5
35	-S-CH_2-CH_2-CO_2H	n.i.	n.d.

The ability of the STLC analogues to induce monoastral spindles raised the possibility that they are able to induce cell cycle arrest in mitosis. To confirm this, we incubated HeLa cells with the analogues for 24 h and we then analyzed the cell-cycle profile of the treated cells by flow cytometry. For the analogues less potent than STLC, we exposed cells with 5 μM and for the more potent we used 1 μM. The histogram profiles are shown in Figure 5, and the % of cells arrested at G2/M with 4 N DNA content is shown in Table 8. Analogues **43** and **59** were less active in arresting cells in G2/M, as it was predicted by their lower EC_{50} values for monoastral spindle formation (Figure 5A; Table 8). The analogues that had slightly worse EC_{50} values for monoastral spindle formation than STLC were able to induce arrest at G2/M at 5 μM (Figure 5A). All the analogues with EC_{50} values for monoastral spindle formation lower than STLC were equally potent (analogues **10** and **48**) or more potent in arresting cell cycle progression at G2/M compared to STLC at 1 μM (Figure 5B; Table 8). Two-

Table 4. K_i^{app} Values for Inhibition of Basal Eg5 ATPase Activity and for Mitotic Arrest Determined Using Cell-Based Assays for Compounds **36–40**

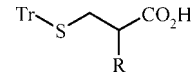

36-40

Compd	R	ATPase activity K_i^{app} [nM]	Cell-based assay EC_{50} [μM]
36	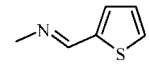	n.i.	> 5
37	-NH-CO-Me	n.i.	n.d.
38	-NH-Tr	n.i.	n.d.
39	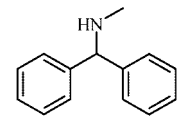	n.i.	n.d.
40	-NH-Boc	n.i.	n.d.

Table 5. K_i^{app} Values for the Inhibition of the Basal Eg5 ATPase Activity and for Induction of Mitotic Arrest for Compounds **41–47**

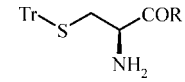

41-47

Compd	R	ATPase activity K_i^{app} [nM]	Cell-based assay EC_{50} [μM]
41[a]	-OMe	120	1.08
42	-$OCH(Ph)_2$	7000	> 5
43[a]	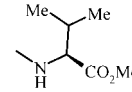	600	3.5
44	-NH-CH_2-CO_2H	1500	> 5
45	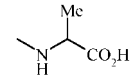	1500	> 5
46[a]	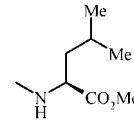	1750	~ 5
47	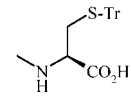	6750	> 5

[a] HCl Salt.

dimensional flow cytometry using the monoclonal antibody MPM2 that recognizes mitosis specific phosphorylated epitopes confirmed that the 4 N arrested cells were indeed mitotic. A total of 86% of the 4 N arrested cells treated with 5 μM STLC were MPM2 positive and thus mitotic. Similarly, 4 N-arrested cells treated with 1 μM of analogues **9**, **50**, **51**, and **52** were 79.9, 77.4, 84.1, and 81.6% MPM2-positive, respectively. Furthermore, the induction of cell cycle arrest in mitosis was analyzed by two-dimensional flow cytometry following 24 h drug exposure in a concentration-dependent manner (Figure 2,

Table 6. K_i^{app} and EC_{50} Values for Inhibition of Basal Eg5 ATPase Activity and for the Induction of Mitotic Arrest in HeLa Cells, Respectively, for Compounds **48–59**

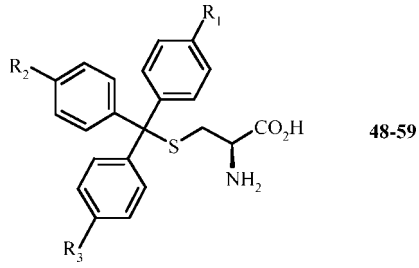

48-59

Cmpd	R_1	R_2	R_3	ATPase activity K_i^{app} [nM]	Cell-based assay EC_{50} [μM]
48	F	H	H	150	1.55
49	Cl	H	H	200	0.51
50	Br	H	H	250	0.31
51	Me	H	H	100	0.21
52	OMe	H	H	200	0.20
53	$-CH_2OH$	H	H	14000	>5
54	OH	H	H	23000	>5
55	Ph	Ph	H	35000	>5
56	OMe	OMe	H	600	>5
57	Me	Me	H	2000	0.53
58	$-CH_2OH$	$-CH_2OH$	H	23000	>5
59	Me	Me	Me	1000	3.1

Table 7. Apparent K_i^{app} and EC_{50} Values for the Inhibition of Basal Eg5 ATPase Activity and for the Induction of Mitotic Arrest, Respectively, for Compounds **60–65**

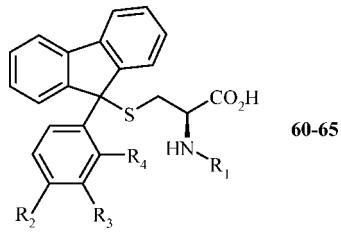

60-65

Cmpd	R_1	R_2	R_3	R_4	ATPase activity K_i^{app} [nM]	Cell-based assay EC_{50} [μM]
60	H	H	H	H	1500	>5
61	H	Me	H	H	13000	>5
62	H	F	H	H	6000	>5
63	H	Cl	H	H	n.i.	>5
64	COMe	H	H	H	n.i.	>5
65	H	H	Ph		900	>5

Supporting Information). The concentration for 50% cells arrested in mitosis and being MPM2 positive was found to be 0.3 μM for compound **52** (Table 8) versus 1.7 μM for STLC (**1**). For compounds **9**, **49**, **50**, **51**, and **52**, the EC_{50} for mitotic arrest were found to be very similar for the EC_{50} values for induction of monoastral spindles (Table 8). In summary, the results suggest that STLC analogues that inhibit Eg5 ATPase activity in in vitro assays also induce monoastral spindles in HeLa cells and lead to cell cycle arrest in mitosis.

Docking and Pharmacophore Modeling. To gain additional insight about the possible binding modes of our STLC derivatives and, also, to be able to explain the results from our SAR studies, we decided to dock some selected compounds from our set into publicly available X-ray crystal structures of Eg5.

So far, 16 experimental structures of 15 different ligands that bind to the allosteric binding-site of Eg5 have been deposited in the PDB database.[25] Overlay of the binding sites from these structures showed that almost all of them share a highly similar binding site conformation (PDB IDs 1II6, 1Q0B, 1X88, 1YRS, 2FKY, 2FL2, 2FL6, 2FME, 2G1Q, 2IEH, 2PG2, 2Q2Y, 2Q2Z, 2UYI, 2UYM). From this set, we chose the structure 2G1Q because the ligand has a $(CH_2)_3NH_2$ side chain that is similar to the $S(CH_2)_2NH_2$ moiety of **31**,[26] and 2FME, whose ligand has a diphenylmethyl substructure, which is also present in our ligands.[27] Recently, a different ligand−protein conformation has been reported (2GM1), which has a larger hydrophobic pocket formed by the rotation of the side chains of Arg101 and Leu196 and which has also a ligand that possesses a $(CH_2)_3NH_2$ side chain.[28] The ligands of the three complexes are depicted in Figure 1.

Compounds **1** (STLC), **2**, **5**, **6**, **8**, **9**, **10**, **15**, **18**, **25**, **28**, **31**, **32**, **33**, **34** (OTLS), **35**, **37**, **41**, **44**, **49**, **51**, **54**, **60**, and **65** were docked with GOLD 3.2 into these three binding sites and scored with the GoldScore function. For compound **1**, we selected both L- and D-stereoisomers, while for the other chiral compounds, only the L-form was investigated. For 19 out of the 25 docked molecules, the highest docking scores could be obtained when using the binding site of 2FME, while for the other six molecules, the binding site of 2GM1 provided the highest scores. For 2G1Q, the scores were considerably lower than for 2FME. The sets of docking poses obtained for each ligand in 2GM1 showed high diversity, making it difficult to derive a preferred binding mode for this type of compound. In many docking trials, the highest scoring conformation was the one where the cysteine part was buried in a hydrophobic pocket that has been shown to be filled by an aromatic moiety in all of the known Eg5 inhibitor complexes. We thus concluded that this larger binding-site conformation is not a likely representation of the complexes that our derivatives form. The most prominent docking pose of our active compounds is shown in Figure 6, exemplified by the highest-scored pose of **51** in 2FME. We used LigandScout 2.0 for visualization of the pharmacophoric interactions between the ligand and the binding side. As can be seen, the three different phenyl groups make hydrophobic interactions at two different pockets and near the opening of the binding site. To be able to better describe the interactions of the different compounds, we termed the hydrophobic interaction sites Hy1, Hy2, and Hy3 (Figure 6, right panel). The primary amino group forms two hydrogen-bond interactions, with oxygen atoms of the carboxylic acid group of Glu 116 and of the backbone carbonyl group of Gly 117. Furthermore, a charged interaction is detected between the protonated amine group and the deprotonated carboxylic acid groups of Glu 116 and Glu 118. The carboxylic acid group of the ligand points outward and does not have any direct interactions with the binding site. The experimental ligand structures of both 2FME and 2G1Q were overlaid with the docked pose of **51** in 2FME, employing the alignment by reference points method (alignment of α-carbon atoms of the binding site amino acids, Figure 3, Supporting Information). It is shown that an aromatic ring is not necessary at Hy1, where the two experimental ligand structures have a planar urea substructure substituted with small aliphatic residues. All three compounds have a phenyl ring at position Hy2 in fairly the same place. 3QC and **51** have phenyl rings positioned at the same position of Hy3, while the aromatic ring of N9H reaches further into this pocket. The amino group of **51** is predicted to interact in the same way as N9H and 2AZ (PDB complex 2GM1, overlay not shown).

Discussion

Compared to tubulin, Eg5 has much more restricted and specific tasks. Mitotic inhibitors specifically acting on Eg5 might

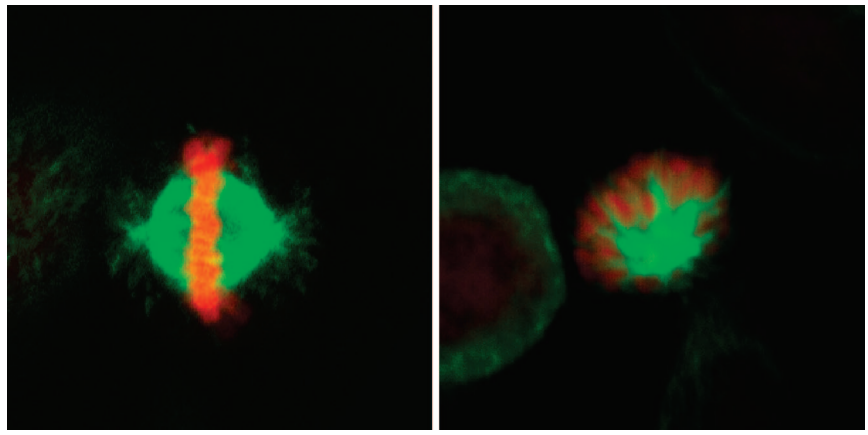

Figure 3. Effect of compound **5** in cell-based assays using HeLa cells. MTs are colored in green, DNA are in red. Left side: HeLa cells in the absence of inhibitors form a bipolar spindle and proceed through mitosis normally. Right side: HeLa cells treated with compound **5** arrest cells in mitosis with a characteristic monoastral spindle phenotype.

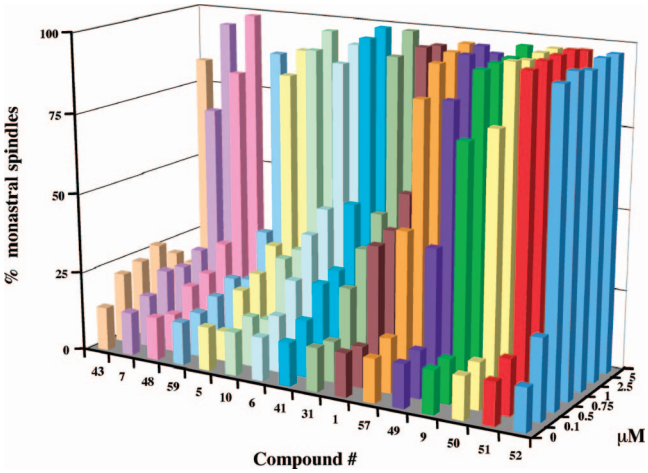

Figure 4. Concentration dependence of induction of monoastral spindles by STLC analogues. HeLa cells after an 8 h exposure to drugs were fixed and stained for immunofluorescence microscopy, as in Figure 3. Mitotic cells were then counted by microscopy, and the cells with monoastral spindles were scored as a percentage of total mitotic cells. Only STLC analogues with an EC_{50} better than 5 μM are shown.

Table 8. Summary of Effects of most Potent STLC Analogues in Cell-Based Assays and FacsScan Analysis

Cmpd	Monoastral spindle formation in HeLa cells EC_{50} [μM]	[%] G2/M 1 μM	[%] G2/M 5 μM	Mitotic arrest in HeLa cells EC_{50} [μM]
1	0.7	23.1	75.8	1.7
5	1.08	19.1	71.1	
6	1.40	22.6	59.1	
7	1.85	19.9	55.2	
9	0.33	68.1	n.d.	0.6
10	1.37	24.3	68	
31	1.08	21.1	65.8	
41	1.08	20.2	72.4	
43	3.5	n.d.	21.8	
48	1.55	24	68.8	
49	0.51	48.5	74.7	0.66
50	0.31	68.7	n.d.	0.45
51	0.21	71	n.d.	0.33
52	0.20	69	n.d.	0.3
57	0.53	50.8	70.9	1
59	3.1	n.d.	34.1	

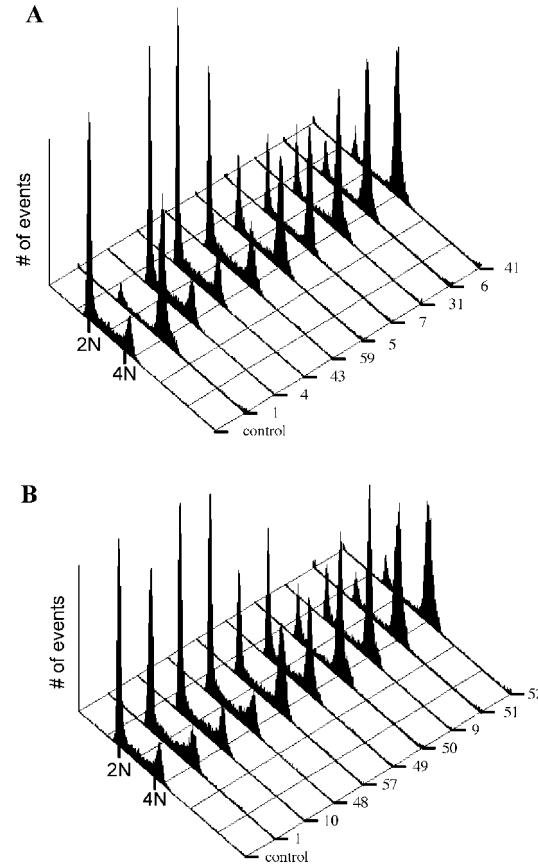

Figure 5. Induction of cell cycle arrest in G2/M phase of the cell cycle after treatment with STLC analogues. Exponentially growing HeLa cells were treated for 24 h with a (A) set of compounds added at 5 μM and a (B) set of compounds that are more potent than STLC (compound **1**) added at 1 μM.

therefore have fewer side effects compared to known tubulin inhibitors. Here we investigated analogues of STLC, a potent inhibitor of Eg5 function that has been previously identified[9] by an in vitro screening procedure and that has been known for some time to induce mitotic arrest without targeting MTs.[15] The interaction of STLC with Eg5 has been studied in vitro and in cell-based assays.[16] STLC is a reversible, tight-binding inhibitor that inhibits basal- and MT-stimulated Eg5 ATPase activity in the low nanomolar range and that hinders MT gliding in motility assays with similar efficacy. The inhibitor binds to a pocket 12 Å away from the ATP binding side, and this pocket is common to most known Eg5 inhibitors so far.[29,30] STLC is an allosteric

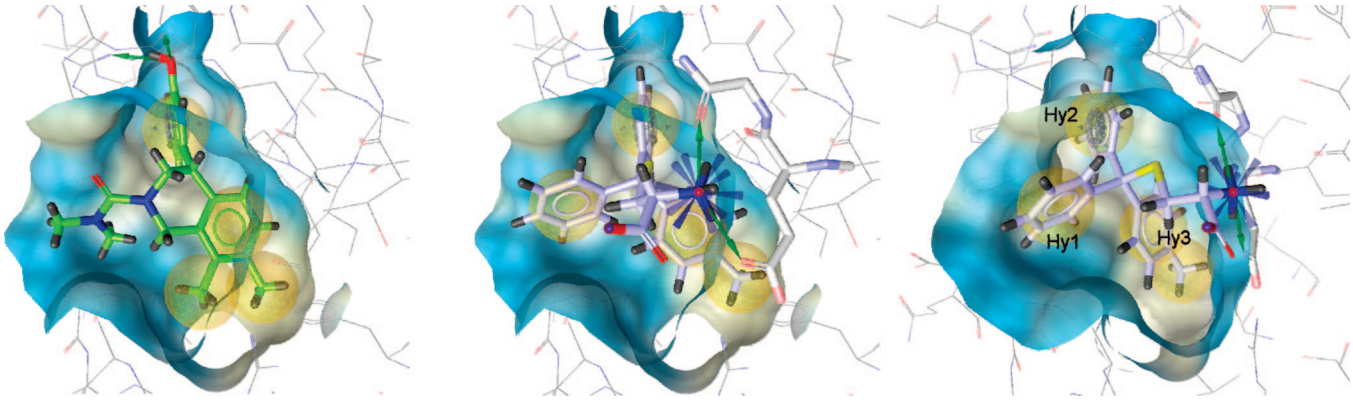

Figure 6. Binding site of ligand 3QC (PDB: 2FME), derived by X-ray crystallography, and putative binding side of compound **51**, derived by docking into the inhibitor binding pocket of Eg5. The binding site surface is colored by aggregated lipophilicity (high, yellow; low, blue). Features showing pharmacophoric interactions between ligand and binding site: yellow spheres, hydrophobic; green arrows, hydrogen bond donor; blue star, positive ionizable/charged; purple ring and arrows, aromatic plane. The numbering of hydrophobic features Hy1 to Hy3 is used in the text to describe the positions of the respective phenyl residues. Compound **51** forms two hydrogen bonds with the side chain oxygen from Glu116 and the main chain oxygen of residue Gly117, which, for clarity, are drawn in white stick representation in the middle and right pictures. Left side: binding pocket of ligand 3QC (PDB: 2FME). Middle: **51** docked into the same binding site. Right side: same docking pose rotated to the right.

inhibitor that inhibits ADP release. In cell-based assays, STLC induces prolonged mitotic arrest[16] in HeLa cells (EC_{50} = 700 nM), which eventually leads to apoptotic cell death.[17] During the onset of mitosis, the duplicated centrosomes fail to fully separate to form the bipolar mitotic spindle and remain locked with a monoastral spindle phenotype. There are no obvious visual affects on interphase cells, even at high STLC concentrations of up to 100 μM. Both in in vitro and in cell-based assays, the *R*- and the *S*-enantiomers of *S*-trityl-cysteine are almost equally potent. We therefore used STLC as a starting point for the synthesis of additional analogues to (i) further narrow down the smallest active pharmacophore responsible for Eg5 inhibition and (ii) to identify more effective analogues. We showed that the cysteine carboxyl group (compound **31**) is not necessary for effective inhibition of Eg5 either in vitro or in cell-based assays, eliminating the necessity for an enantioselective synthesis of STLC analogues. *S*-Diphenyl-L-cysteine (**2**) is inactive, whereas alkyl compound intermediates become increasingly active in vitro (**3**−**7**) and in cell-based assays. Thus, of all STLC analogues tested in this study, **31** represents the smallest active compound. However, the cell-based inhibition activity could be improved by introducing halogene or alkyl ligands in the *para*-position of the three phenyl groups (Table 6), leading to K_i^{app} values in HeLa cells of about 200 nM, representing increased activities in cell-based assays.

Structurally Related Analogues and their Use as Potential Anticancer Targets. One recent patent discloses triphenylmethane compounds as inhibitors of Eg5 activity,[31] including molecules with substitutions in *ortho*-, *meta*-, and *para*-positions of the phenyl rings. The cysteine ligand present in our inhibitors is exchanged with either hydrogen or lower alkyl chains, indicating that triphenylalkyl compounds without sulfur are also capable of inhibiting Eg5 activity. However, IC_{50} values and the effectiveness of these analogues are not given, thus making a direct comparison difficult. Another study identified triphenylmethylamides that arrest melanoma cells in G1 of the cell cycle[32] subsequently inducing apoptosis. The *S*-triphenyl compounds characterized in our study also eventually lead to apoptosis, however, after a prolonged mitotic arrest in M-phase, indicating that different proteins are probably targeted by these two distinct types of compounds.

Interpretation of SAR Results Based on Docking Studies. The fact that the carboxylic acid group points to the outside of the binding pocket explains why there was no stereoselectivity found for **1**. While the docking results were not really clear on that, from a comparison with other compounds in the literature we would expect the aliphatic residues of **3**−**7** to be positioned at Hy1. The β-naphthyl group of **9** nicely fits into Hy3, reaching the same space that is covered by the difluorophenyl group of N9H, while the α-naphthyl group of **8** does not fit this pocket. The 1,3-benzodioxole group of **10** was placed at all three different positions, although we would expect it to bind in the same way as **9**. Interestingly, there are many known inhibitors of Eg5 that do not have a primary amino group and still have good affinity, while this seems to be a prerequisite for the derivatives of STLC, as shown by compounds of Tables 2 and 3. Also, for most compounds of Tables 3−5, visual inspection of the binding poses as well as the obtained GoldScore values are in good agreement with the experimental values obtained. For example, the lower K_i^{app} value of the oxy-analogue OTLS was reflected by its lower GoldScore value, pointing out the favorable effect of the sulfur group at this position. Surprisingly, the highest docking scores of all investigated compounds were obtained for **44** (92.95 vs 83.70 for **1** and 88.38 for **49**). The proposed binding mode shows additional interactions between the glycine carboxylic acid group of the ligand and Arg 221. So far, we cannot explain the reduced affinity of this ligand. The proposed binding mode of the amino group of our compounds explains why it is important that the positive charge as well as the possibility to form two hydrogen bonds is retained. Recently reported compounds of another group show that, in their series, replacement of the primary amino group by small tertiary amino groups is tolerated, leading to compounds with similar affinity.[33] Experimental data for such compounds shows that the amino group bearing aliphatic chain moves away from the protein, losing the two hydrogen bonds while retaining the charged interactions (PDB codes 2Q2Y, 2Q2Z).[34] Compounds from Table 6 were docked into the binding site of 2FME to gain insight about the possible placement of the substituted phenyl rings inside the binding pocket. Regardless of hydrophobicity of the substituents, Hy3 was occupied by R_1 of most singly substituted derivatives (**48**−**54**), except for **55**, which seems to be too big to occupy this pocket. Compounds **56**−**58** possess two *para*-substituted phenyl residues, which were placed at both Hy3 and Hy1, while the derivative with three substituents accessed all three hydrophobic interaction points. Despite equal or higher GoldScore values, both hydrophilic (**53**, **54**, and **58**) and bulky (**55**) groups,

as well as *para*-substitution at the second and third phenyl ring (**56**-**59**), diminish affinity. For **60**, we received poses where the two connected phenyl rings of the fluorene system cover Hy1 and Hy3, while the free phenyl ring reaches into Hy2. It has been shown in other studies that this binding pocket is rather small, which explains the lower affinity of **61**−**63**, when the influence of the same substituents in **48**, **49**, and **51** was neutral to positive; as stated above, for these compounds, the residues can access Hy3. From these results, we would expect the bulky compound **65** to be inactive as well, although it showed somewhat better inhibition of ATPase activity than **60**. We obtained different kinds of docking poses but are yet unable to explain the observed affinity for this compound.

Conclusion

We have performed an initial structure–activity relationship of STLC analogues, potent inhibitors of human mitotic Eg5 that lead to prolonged mitotic arrest and subsequent cell death. The most potent analogues are tight-binding Eg5 inhibitors in vitro, with an estimated K_i^{app} of about 100 nM, that induce mitotic arrest in HeLa cells, with an EC_{50} of about 200 nM. The docking studies we performed proposed ligand conformations that are in good agreement with the SAR data obtained for our compounds. This perception of the likely binding modes of our compounds enables us to further pursue the design of analogues with improved potency to inhibit Eg5.

Experimental Section

Chemistry. Melting points were obtained with a Büchi capillary apparatus and are uncorrected. Optical rotations were measured at the sodium D line (589 nm) at room temperature with a Perkin-Elmer 241 polarimeter using a 1 dm path length cell. ^{1}H and ^{13}C NMR spectra were recorded on a Bruker Avance 300 MHz spectrometer. Chemical shifts are reported in ppm (δ) relative to tetramethylsilane (TMS) as an internal standard. Multiplicities are given as s (singlet), d (doublet), dd (double–doublet), q (quadruplet), t (triplet), and m (multiplet). Mass spectra were recorded with a Perkin-Elmer SCIEX API spectrometer using ionspray methodology. Elemental analyses were performed on a Thermoquest Flash 1112 series EA analyzer. Elemental compositions of the compounds agreed to within 0.4% of the calculated value. Thin layer chromatography (TLC) was conducted on aluminum sheet silica gel Merck $60F_{254}$. The spots were visualized using an ultraviolet light. Flash chromatography was carried out on silica gel 60 (40–63 μm, Merck) using the indicated solvents (petroleum ether (PE): boiling range 40–60 °C). All reactions requiring anhydrous conditions were conducted in flame-dried apparatus. All commercially available reagents and solvents were used without further purification. Compounds **1**, **2**, **8**–**31**, and **35**–**65** were obtained from the Drug Synthesis and Chemistry Branch, Developmental Therapeutics Program, Division of Cancer Treatment and Diagnosis, National Cancer Institute, U.S.A. The other compounds were synthesized as follows.

General Procedure for Preparation of Compounds 3–7. At 0 °C and under an argon atmosphere, a solution of $BF_3 \cdot Et_2O$ (0.82 mmol) was added dropwise to a solution of alcohols (0.55 mmol), L-cysteine (0.48 mmol) in AcOH (0.5 mL). The reaction mixture was stirred at room temperature for 2 h. Addition of a 10% NaOAc solution (1.5 mL), then H_2O (1.5 mL) led to the precipitation of **3**, **4**, and **6**. After filtration, final compounds **3**, **4**, and **6** were obtained as white solids. For **5** and **7**, the products were extracted from the final solution with Et_2O (2 × 10 mL). The combined organic layers were dried over $MgSO_4$. The solvent was removed under reduced pressure and the crude residue was purified by flash chromatography (eluent CH_2Cl_2/MeOH 9:1) to afford **5** and **7** as white solids.

***S*-(1,1-Diphenylethyl)-L-cysteine (3).** Alcohol = 1,1-diphenylethanol.[19,20] Yield: 69%. Mp 175–177 °C (lit:[21] 178 °C). $[\alpha]^{20}_D$ +8.6° (*c* 0.5, MeOH) [lit:[21] +34.0° (*c* 2.0, 0.1 M HCl in EtOH)]. ^{1}H NMR (300 MHz, CD_3OD + D_2O): δ 2.12 (s, 3H, CH_3), 2.69 (dd, 1H, J = 9.5, 13.5 Hz, CH_2), 2.95 (dd, 1H, J = 3.8, 13.5 Hz, CH_2), 3.25 (dd, 1H, J = 3.8, 9.5 Hz, CH), 7.21–7.34 (m, 6H, H_{Ar}), 7.42–7.47 (m, 4H, H_{Ar}). MS: *m*/*z* 302 (M^+ + 1).

***S*-(1,1-Diphenylpropyl)-L-cysteine (4).** Alcohol = 1,1-diphenylpropanol.[19,20] Yield: 37%. Mp 180–182 °C. $[\alpha]^{20}_D$ +12.0° (*c* 0.5, MeOH). ^{1}H NMR (300 MHz, CD_3OD + D_2O): δ 0.80 (t, 3H, J = 7.1 Hz, CH_3), 2.46 (q, 2H, J = 7.1 Hz, CH_2), 2.54 (dd, 1H, J = 9.6, 13.6 Hz, CH_2), 2,82 (dd, 1H, J = 3.6, 13.6 Hz, CH_2), 3.03 (dd, 1H, J = 3.6, 9.6 Hz, CH), 7.22–7.43 (m, 10H, H_{Ar}). MS: *m*/*z* 316 (M^+ + 1).

***S*-(1,1-Diphenylpentyl)-L-cysteine (5).** Alcohol = 1,1-diphenylpentanol.[19,20] Yield: 39%. Mp 154–156 °C. $[\alpha]^{20}_D$ +5.1° (*c* 0.5, MeOH). ^{1}H NMR (300 MHz, CD_3OD + D_2O): δ 0.83 (t, 3H, J = 7.2 Hz, CH_3), 1.12–1.21 (m, 2H, CH_2), 1.24–1.34 (m, 2H, CH_2), 2.42 (broad t, 2H, J = 8.1 Hz, CH_2), 2.56 (dd, 1H, J = 9.8, 13.6 Hz, CH_2), 2.85 (dd, 1H, J = 3.7, 13.6 Hz, CH_2), 2.98 (dd, 1H, J = 3.7, 9.8 Hz, CH), 7.21–7.43 (m, 10H, H_{Ar}). MS: *m*/*z* 344 (M^+ + 1).

***S*-(2-Methyl-1,1-diphenylpropyl)-L-cysteine (6).** Alcohol = 2-methyl-1,1-diphenylpropanol.[19,20] Yield: 62%. Mp 165–167 °C. $[\alpha]^{20}_D$ +18.5° (*c* 0.5, MeOH). ^{1}H NMR (300 MHz, CD_3OD + D_2O): δ 0.89 (d, 3H, J = 6.6 Hz, CH_3), 0.95 (d, 3H, J = 6.6 Hz, CH_3), 2.52 (dd, 1H, J = 9.8, 13.6 Hz, CH_2), 2.73 (dd, 1H, J = 3.8, 13.6 Hz, CH_2), 2.82 (dd, 1H, J = 3.8, 9.8 Hz, CH), 2.99–3.08 (m, 1H, CH), 7.24–7.50 (m, 10H, H_{Ar}). MS: *m*/*z* 330 (M^+ + 1).

***S*-[Cyclohexyl(diphenyl)methyl]-L-cysteine (7).** Alcohol = cyclohexyldiphenylmethanol.[19,20] Yield: 25%. Mp 152–154 °C; $[\alpha]^{20}_D$ +12.9° (*c* 0.25, MeOH). ^{1}H NMR (300 MHz, CD_3OD + D_2O): δ 0.51–0.97 (m, 3H, CH_3), 1.34–1.47 (m, 2H, CH_2), 1.61–1.78 (m, 3H, CH_2), 2.12–2.18 (m, 2H, CH_2), 2.48 (dd, 1H, J = 9.8, 13.6 Hz, CH_2), 2.49–2.60 (m, 1H, CH_2), 2.70 (dd, 1H, J = 3.7, 13.6 Hz, CH_2), 2.79 (dd, 1H, J = 3.7, 9.8 Hz, CH), 7.23–7.47 (m, 10H, H_{Ar}). MS: *m*/*z* 370 (M^+ + 1).

3-(Tritylmercapto)propylamine (32). To a solution of tritylmercaptan (553 mg, 2.0 mmol) in dry DMF (5 mL), sodium hydride 60% (106 mg, 4.4 mmol) was added at 0 °C. The reaction mixture was stirred at 0 °C for 10 min. A solution of bromopropylamine hydrobromide (438 mg, 2.0 mmol) in dry DMF (2.5 mL) was added dropwise. The final mixture was stirred overnight at room temperature. After addition of H_2O (10 mL) and EtOAc (10 mL) to the solution, the product was extracted. The organic layer was dried over $MgSO_4$. The solvent was removed under reduced pressure and the crude residue was purified by flash chromatography (eluent CH_2Cl_2/MeOH 95:05) to afford **32** (550 mg, 82%) as an oil, which crystallized slowly in the refrigerator; Mp 54–56 °C. ^{1}H NMR (300 MHz, $CDCl_3$): δ 1.48–1.57 (m, 2H, CH_2), 2.20 (t, 2H, J = 7.3 Hz, CH_2), 2.63 (t, 2H, J = 6.8 Hz, CH_2), 7.18–7.31 (m, 9H, H_{Ar}), 7.40–7.43 (m, 6H, H_{Ar}). MS: *m*/*z* 334 (M^+ + 1).

4-(Tritylmercapto)butylamine (33). To a solution of trityl mercaptan (277 mg, 1.0 mmol) in dry DMF (5 mL), sodium hydride 60% (27 mg, 1.1 mmol) was added at 0 °C. The reaction mixture was stirred at 0 °C for 30 min. A solution of bromobutylphthalimide (311 mg, 1.1 mmol) in dry DMF (5 mL) was added dropwise. The final mixture was stirred overnight at room temperature. After addition of H_2O (10 mL) and EtOAc (10 mL) to the solution, the product was extracted. The organic layer was dried over $MgSO_4$. The solvent was removed under reduced pressure and the crude residue was purified by flash chromatography (eluent PE/EtOAc 8:2) to afford phthalimido-*S*-trityl intermediate (380 mg, 85%) as a solid. Mp 100–102 °C (EtOH; lit:[22] 120–123 °C). ^{1}H NMR (300 MHz, $CDCl_3$): δ 1.33–1.43 (m, 2H, CH_2), 1.57–1.67 (m, 2H, CH_2), 2.17 (t, 2H, J = 7.5 Hz, CH_2), 3.56 (t, 2H, J = 7.5 Hz, CH_2), 7.15–7.28 (m, 9H, H_{Ar}), 7.38–7.41 (m, 6H, H_{Ar}), 7.69–7.74 (m, 2H, H_{Ar}), 7.81–7.84 (m, 2H, H_{Ar}). To a suspended solution of phthalimido-*S*-trityl intermediate (150 mg, 0.31 mmol) in EtOH/*n*-BuOH (12 mL, 5:1 v/v), hydrazine monohydrate (0.1 mL, 2.08 mmol) was added. The mixture was stirred at 50 °C for 2 h. After cooling, the resulting precipitate was removed by filtration and the filtrate was collected and evaporated in vacuo. Then chloroform was added to the resulting residue and the mixture was stirred for

45 min. The mixture was filtered, and the filtrate was collected was evaporated in vacuo. The crude product was purified by flash chromatography (eluent CH_2Cl_2/MeOH 9:1) to afford **33** (80 mg, 74%) as an oil, which crystallized from $CHCl_3$. Mp 48–50 °C ($CHCl_3$). ^{1}H NMR (300 MHz, $CDCl_3$): δ 1.34–1.50 (m, 4H, CH_2), 2.16 (t, 2H, $J = 6.8$ Hz, CH_2), 2.61 (t, 2H, $J = 6.8$ Hz, CH_2), 3.67 (broad s, 2H, NH_2), 7.18–7.30 (m, 9H, H_{Ar}), 7.39–7.42 (m, 6H, H_{Ar}). MS: m/z 348 ($M^+ + 1$).

***O*-(Trityl)-L-serine (34).** Following the procedure described for **3**, **4**, and **6**, the compound **34** was prepared from L-serine and triphenylmethanol in 30% yield as a solid (time reaction = 4 h, room temperature). Mp 170–172 °C (washing Et_2O; lit:[23] 208–209 °C). $[\alpha]^{20}_D$ −9.7° [*c* 0.5, MeOH; lit:[23] $[\alpha]^{20}_D$ +8.3° (*c* 2.0, 0.1 N NaOH)]. ^{1}H NMR (300 MHz, $CD_3OD + D_2O$): δ 3.50 (dd, 1H, $J = 3.2$, 10.0 Hz, CH_2), 3.60 (dd, 1H, $J = 6.0$, 10.0 Hz, CH_2), 3.68 (dd, 1H, $J = 3.2$, 6.0 Hz, CH), 7.22–7.35 (m, 9H, H_{Ar}), 7.46–7.49 (m, 6H, H_{Ar}). MS: m/z 348 ($M^+ + 1$).

Determination of IC_{50} Values by Inhibition of Basal Eg5 ATPase Activity. The inhibition of Eg5 ATPase activity (K_i^{app} values) was quantified as previously described.[16] All analogues were measured once (IC_{50}) to separate compounds that inhibit basal Eg5 activity from those that do not (molecules that retain between 80% to 100% of the initial activity). In a second step, the inhibition of basal Eg5 activity of active compounds was measured in triplicate at the same time, employing at least two different Eg5 concentrations and displayed with standard deviations. The best inhibiting compound of each table was used to estimate its apparent K_i value (K_i^{app}) from four different protein concentrations by fitting the data to the Morrison equation, as previously described.[16,35] Estimates of the K_i^{app} values can vary, depending on the buffer and test conditions used.

Cells and Culture Conditions. HeLa cells were grown on Dulbecco's modified Eagle's medium (GIBCO, BRL), supplemented with 10% fetal bovine serum (Hyclone), and maintained in a humid incubator at 37 °C in 5% CO_2. Cells were seeded and left to adhere for at least 36 h on poly-D-lysine-coated glass coverslips in 24-well plates. Drugs were diluted appropriately in medium from 50 mM stocks in 100% DMSO and then added to the cells. Following 7 h incubation with drugs, cells were fixed with 1% paraformaldehyde-PBS at 37 °C for 3 min, followed by a 5 min incubation in 100% methanol at –20 °C. Coverslips were then washed with PBS, and the cells were stained with anti-β-tubulin monoclonal antibodies for 1 h and then with an FITC-conjugated goat antimouse secondary antibody (Jakson ImmunoResearch Laboratories, West Grove, PA) for 30 min and counterstained with propidium iodide. EC_{50} values for the quantification of cells in mitotic arrest over the total number of mitotic cells were determined as previously described.[16] The percentage of mitotic cells with monoastral spindles present in treated cells was calculated over the total number of cells in mitosis counted after 8 h incubation with drugs. Images were collected with a MRC-600 Laser Scanning Confocal apparatus (BioRAD Laboratories) coupled to a Nikon Optiphot microscope.

Cell Cycle Analysis by Flow Cytometry (FACS). Cells grown in 60 mm dishes were treated with drugs for 24 h and, following fixation, were analyzed by two-dimensional flow cytometry using MPM-2, a mitotic marker, and propidium iodide, a marker of DNA content. Cells were fixed in 90% methanol at –20 °C for at least 10 min and, following three washes with PBS, were incubated with MPM-2 monoclonal antibody (Upstate, Lake Placid, NY) and labeled with FITC-conjugated antimouse IgG secondary antibodies (Jackson laboratories, West Grove, PA) and propidium iodide, as described previously. Data were collected using a FACScan flow cytometer (Becton Dickinson, San Jose, CA) using Cellquest software, with propidium iodide in the first and MPM-2 in the second dimension. For each sample, 10000 events were collected and aggregated cells were gated out.

Molecular Modeling. All docking calculations were performed on a PC equipped with a 2.13 GHz Core 2 Duo processor and 1 GB of RAM, running Fedora Core 6 Linux. Ligands were drawn and minimized in the protonation states that are present at physiological pH value (protonated amino groups, deprotonated carboxylic acid groups) within Catalyst 4.11.[36] The binding sites were prepared for docking in Sybyl 7.2.[37] Docking studies were performed with GOLD 3.2.[38] All waters present in the binding site were allowed to be replaced by the ligand or to change their orientation. All other settings were kept at their default values. LigandScout 2.0 was used for visual inspection of the docked poses, generation of pharmacophore models, and overlay of the ligands, as depicted in Figure 6.[39]

Acknowledgment. We thank the National Cancer Institute/National Institutes of Health (Drug Synthesis and Chemistry Branch, Developmental Therapeutics Program, Division of Cancer Treatment and Diagnosis) for providing us with many of the *S*-trityl-L-cysteine analogues used in this study. This work has been funded by grants from ARC (Association pour la Recherche sur le Cancer, Contract No. 3973).

Supporting Information Available: Figure 1, characterization of STLC analogues as tight-binding inhibitors of human Eg5; Figure 2, induction of cell cycle arrest in mitosis by STLC analogues; Figure 3, overlay of X-ray crystal ligands 3QC, N9H, and the highest scored docking pose of **51** in 2FME; Table 1, compound numbering, as indicated in the manuscript, and corresponding NSC numbers; Table 2, highest GoldScore values for compounds that were docked into the three binding sites; and Table 3, elemental analyses of compounds **3**−**7** and **32**−**34**. This material is available free of charge via the Internet at http://pubs.acs.org.

References

(1) Zhu, C.; Zhao, J.; Bibikova, M.; Leverson, J. D.; Bossy-Wetzel, E.; Fan, J. B.; Abraham, R. T.; Jiang, W. Functional analysis of human microtubule-based motor proteins, the kinesins and dyneins, in mitosis/cytokinesis using RNA interference (RNAi). *Mol. Biol. Cell* **2005**, *16*, 3187–3199.

(2) Wood, K. W.; Cornwell, W. D.; Jackson, J. R. Past and future of the mitotic spindle as an oncology target. *Curr. Opin. Pharmacol.* **2001**, *1*, 370–377.

(3) Miyamoto, D. T.; Perlman, Z. E.; Mitchison, T. J.; Shirasu-Hiza, M. Dynamics of the mitotic spindle–potential therapeutic targets. *Prog. Cell Cycle Res.* **2003**, *5*, 349–360.

(4) Bergnes, G.; Brejc, K.; Belmont, L. Mitotic kinesins: prospects for antimitotic drug discovery. *Curr. Top. Med. Chem.* **2005**, *5*, 127–145.

(5) Blangy, A.; Lane, H. A.; d'Herin, P.; Harper, M.; Kress, M.; Nigg, E. A. Phosphorylation by $p34^{cdc2}$ regulates spindle association of human Eg5, a kinesin-related motor essential for bipolar spindle formation in vivo. *Cell* **1995**, *83*, 1159–1169.

(6) Mayer, T. U.; Kapoor, T. M.; Haggarty, S. J.; King, R. W.; Schreiber, S. L.; Mitchison, T. J. Small molecule inhibitor of mitotic spindle bipolarity identified in a phenotype-based screen. *Science* **1999**, *286*, 971–974.

(7) Nakazawa, J.; Yajima, J.; Usui, T.; Ueki, M.; Takatsuki, A.; Imoto, M.; Toyoshima, Y. Y.; Osada, H. A novel action of terpendole E on the motor activity of mitotic kinesin Eg5. *Chem. Biol.* **2003**, *10*, 131–137.

(8) Hotha, S.; Yarrow, J. C.; Yang, J. G.; Garrett, S.; Renduchintala, K. V.; Mayer, T. U.; Kapoor, T. M. HR22C16: A potent small-molecule probe for the dynamics of cell division. *Angew. Chem., Int. Ed.* **2003**, *42*, 2379–2382.

(9) DeBonis, S.; Skoufias, D.; Robin, G.; Lebeau, L.; Lopez, R.; Margolis, R.; Wade, R. H.; Kozielski, F. In vitro screening for inhibitors of the human mitotic kinesin, Eg5, with antimitotic and antitumor activity. *Mol. Cancer Ther.* **2004**, *3*, 1079–1090.

(10) Sakowicz, R.; Finer, J. T.; Beraud, C.; Crompton, A.; Lewis, E.; Fritsch, A.; Lee, Y.; Mak, J.; Moody, R.; Turincio, R.; Chabala, J. C.; Gonzales, P.; Roth, S.; Weitman, S.; Wood, K. W. Antitumor activity of a kinesin inhibitor. *Cancer Res.* **2004**, *64*, 3276–3280.

(11) Gartner, M.; Sunder-Plassmann, N.; Seiler, J.; Utz, M.; Vernos, I.; Surrey, T.; Giannis, A. Development and biological evaluation of potent and specific inhibitors of mitotic kinesin Eg5. *ChemBioChem* **2005**, *6*, 1173–1177.

(12) Sunder-Plassmann, N.; Sarli, V.; Gartner, M.; Utz, M.; Seiler, J.; Huemmer, S.; Mayer, T. U.; Surrey, T.; Giannis, A. Synthesis and biological evaluation of new tetrahydro-beta-carbolines as inhibitors of the mitotic kinesin Eg5. *Bioorg. Med. Chem.* **2005**, *13*, 6094–6111.

(13) Tao, W.; South, V. J.; Zhang, Y.; Davide, J. P.; Farrel, L.; Kohl, N. E.; Sepp-Lorenzino, L.; Lobell, R. B. Induction of apoptosis by an inhibitor of the mitotic kinesin KSP requires both activation of the spindle assembly checkpoint and mitotic slippage. *Cancer Cell* **2005**, *8*, 49–59.

(14) Cox, C. D.; Breslin, M. J.; Mariano, B. J.; Coleman, P. J.; Buser, C. A.; Walsh, E. S.; Hamilton, K.; Huber, H. E.; Kohl, N. E.; Torrent, M.; Yan, Y.; Kuo, L. C.; Hartman, G. D. Kinesin spindle protein (KSP) inhibitors. Part 1: The discovery of 3,5-diaryl-4,5-dihydropyrazoles as potent and selective inhibitors of the mitotic kinesin KSP. *Bioorg. Med. Chem. Lett.* **2005**, *15*, 2041–2045.

(15) Paull, K. D.; Lin, C. M.; Malspeis, L.; Hamel, E. Identification of novel antimitotic agents at the tubulin level by computer-assisted evaluation of differential cytotoxicity data. *Cancer Res.* **1992**, *52*, 3892–3900.

(16) Skoufias, D. A.; Debonis, S.; Lebeau, L.; Crevel, I.; Cross, R.; Wade, R. H.; Hackney, D. D.; Kozielski, F. *S*-Trityl-L-cysteine is a reversible, tight binding inhibitor of human Eg5 that specifically blocks mitotic progression. *J. Biol. Chem.* **2006**, *281*, 17559–17569.

(17) Xiao, D.; Pinto, J. T.; Gunderson, G. F.; Weinstein, I. B. Effects of a series of organosulfur compounds on mitotic arrest and induction of apoptosis in colon cancer cells. *Mol. Cancer Ther.* **2005**, *4*, 1388–1398.

(18) Brier, S.; Lemaire, D.; DeBonis, S.; Forest, E.; Kozielski, F. Identification of the binding region of a new potent inhibitor of the mitotic kinesin Eg5. *Biochemistry* **2004**, *43*, 13072–13082.

(19) (a) Guijarro, D.; Mancheno, B; Yus, M. C-O dilithiated diarylmethanols: Easy and improved preparation by naphthalene-catalysed lithiation of diaryl ketones and reactivity toward electrophiles. *Tetrahedron* **1993**, *49*, 1327–1334. (b) Guijarro, D.; Guillena, G.; Mancheno, B; Yus, M. Direct transformation of dialkyl sulfates into alkyllithium reagents by a naphthalene-catalysed lithiation. *Tetrahedron* **1994**, *50*, 3427–3436.

(20) (a) Hatano, M.; Matsumura, T.; Ishihara, K. Highly alkyl-selective addition to ketones with magnesium ate complexes derived from Grignard reagents. *Org. Lett.* **2005**, *7*, 573–576. (b) Hatano, M.; Suzuki, S.; Ishihara, K. Highly efficient alkylation to ketones and aldimines with Grignard reagents catalyzed by zinc(II) chloride. *J. Am. Chem. Soc.* **2006**, *128*, 9998–9999.

(21) Koenig, W.; Geiger, R.; Siedel, W. New sulfur protective groups for cysteine. *Chem. Ber.* **1968**, *101*, 681–699.

(22) Gazal, S.; Gellerman, G.; Glukhov, E.; Gilon, C. Synthesis of novel protected N^{α}(ω-thioalkyl)amino acid building units and their incorporation in backbone cyclic disulfide and thioetheric bridged peptides. *J. Pept. Res.* **2001**, *58*, 527–539.

(23) Zee-Cheng, K.-Y.; Cheng, C. C. Experimental antileukemic agents. Preparation and structure-activity study of *S*-tritylcysteine and related compounds. *J. Med. Chem.* **1970**, *13*, 414–418.

(24) Ogo, N.; Oishi, S.; Matsuno, K.; Sawada, J.; Fujii, N.; Asai, A. Synthesis and biological evaluation of L-cysteine derivatives as mitotic kinesin inhibitors. *Bioorg. Med. Chem. Lett.* **2007**, *17*, 3921–3924.

(25) Berman, H. M.; Westbrook, J.; Feng, Z.; Gilliland, G.; Bhat, T. N.; Weissig, H.; Shindyalov, I. N.; Bourne, P. E. The Protein Data Bank. *Nucleic Acids Res.* **2000**, *28*, 235–242.

(26) Cox, C. D.; Torrent, M.; Breslin, M. J.; Mariano, B. J.; Whitman, D. B.; Coleman, P. J.; Buser, C. A.; Walsh, E. S.; Hamilton, K.; Schaber, M. D.; Lobell, R. B.; Tao, W.; South, V. J.; Kohl, N. E.; Yan, Y.; Kuo, L. C.; Prueksaritanont, T.; Slaughter, D. E.; Li, C.; Mahan, E.; Lu, B.; Hartman, G. D. Kinesin spindle protein (KSP) inhibitors. Part 4: Structure-based design of 5-alkylamino-3,5-diaryl-4,5-dihydropyrazoles as potent, water-soluble inhibitors of the mitotic kinesin KSP. *Bioorg. Med. Chem. Lett.* **2006**, *16*, 3175–3179.

(27) Tarby, C. M.; Kaltenbach, R. F., 3rd; Huynh, T.; Pudzianowski, A.; Shen, H.; Ortega-Nanos, M.; Sheriff, S.; Newitt, J. A.; McDonnell, P. A.; Burford, N.; Fairchild, C. R.; Vaccaro, W.; Chen, Z.; Borzilleri, R. M.; Naglich, J.; Lombardo, L. J.; Gottardis, M.; Trainor, G. L.; Roussell, D. L. Inhibitors of human mitotic kinesin Eg5: Characterization of the 4-phenyl-tetrahydroisoquinoline lead series. *Bioorg. Med. Chem. Lett.* **2006**, *16*, 2095–2100.

(28) Kim, K. S.; Lu, S.; Cornelius, L. A.; Lombardo, L. J.; Borzilleri, R. M.; Schroeder, G. M.; Sheng, C.; Rovnyak, G.; Crews, D.; Schmidt, R. J.; Williams, D. K.; Bhide, R. S.; Traeger, S. C.; McDonnell, P. A.; Mueller, L.; Sheriff, S.; Newitt, J. A.; Pudzianowski, A. T.; Yang, Z.; Wild, R.; Lee, F. Y.; Batorsky, R.; Ryder, J. S.; Ortega-Nanos, M.; Shen, H.; Gottardis, M.; Roussell, D. L. Synthesis and SAR of pyrrolotriazine-4-one based Eg5 inhibitors. *Bioorg. Med. Chem. Lett.* **2006**, *16*, 3937–3942.

(29) Yan, Y.; Sardana, V.; Xu, B.; Homnick, C.; Halczenko, W.; Buser, C. A.; Schaber, M.; Hartman, G. D.; Huber, H. E.; Kuo, L. C. Inhibition of a mitotic motor protein: Where, how, and conformational consequences. *J. Mol. Biol.* **2003**, *335*, 547–554.

(30) Garcia-Saez, I.; DeBonis, S.; Lopez, R.; Trucco, F.; Rousseau, B.; Thuéry, P.; Kozielski, F. Structure of human Eg5 in complex with a new monastrol-based inhibitor bound in the (*R*)-configuration. *J. Biol. Chem.* **2007**, *282*, 9740–9747.

(31) Finer, J. T.; Chabala, J. C.; Lewis, E. Preparation of triphenylmethane as kinesin KSP inhibitors. PCT Int. Appl. WO 02/056880 A1. **2002**; *Chem. Abstr. 137*, 124985.

(32) Dothager, R. S.; Putt, K. S.; Allen, B. J.; Leslie, B. J.; Nesterenko, V.; Hergenrother, P. J. Synthesis and identification of small molecules that potently induce apoptosis in melanoma cells through G1 cell cycle arrest. *J. Am. Chem. Soc.* **2005**, *127*, 8686–8696.

(33) Coleman, P. J.; Schreier, J. D.; Cox, C. D.; Fraley, M. E.; Garbaccio, R. M.; Buser, C. A.; Walsh, E. S.; Hamilton, K.; Lobell, R. B.; Rickert, K.; Tao, W.; Diehl, R. E.; South, V. J.; Davide, J. P.; Kohl, N. E.; Yan, Y.; Kuo, L.; Prueksaritanont, T.; Li, C.; Mahan, E. A.; Fernandez-Metzler, C.; Salata, J. J.; Hartman, G. D. Kinesin spindle protein (KSP) inhibitors. Part 6: Design and synthesis of 3,5-diaryl-4,5-dihydropyrazole amides as potent inhibitors of the mitotic kinesin KSP. *Bioorg. Med. Chem. Lett.* **2007**, *17*, 5390–5395.

(34) Roecker, A. J.; Coleman, P. J.; Mercer, S. P.; Schreier, J. D.; Buser, C. A.; Walsh, E. S.; Hamilton, K.; Lobell, R. B.; Tao, W.; Diehl, R. E.; South, V. J.; Davide, J. P.; Kohl, N. E.; Yan, Y.; Kuo, L. C.; Li, C.; Fernandez-Metzler, C.; Mahan, E. A.; Prueksaritanont, T.; Hartman, G. D. Kinesin spindle protein (KSP) inhibitors. Part 8: Design and synthesis of 1,4-diaryl-4,5-dihydropyrazoles as potent inhibitors of the mitotic kinesin KSP. *Bioorg. Med. Chem. Lett.* **2007**, *17*, 5677–5682.

(35) Brier, S.; Lemaire, D.; DeBonis, S.; Forest, E.; Kozielski, F. Molecular dissection of the inhibitor binding pocket of mitotic kinesin Eg5 reveals mutants that confer resistance to antimitotic agents. *J. Mol. Biol.* **2006**, *360*, 360–376.

(36) *Catalyst 4.11*; Accelrys: San Diego, CA, 2005.

(37) *Sybyl 7.2*; Tripos, Inc.: St. Louis, MO, 2006.

(38) *Gold 3.2*; The Cambridge Crystallographic Data Centre: Cambridge, U.K., 2007.

(39) (a) Wolber, G.; Dornhofer, A.; Langer, T. Efficient overlay of small molecules using 3-D pharmacophores. *J. Comput.-Aided. Mol. Des.* **2006**, *20*, 773–788. (b) Wolber, G.; Langer, T. LigandScout: 3D pharmacophores derived from protein-bound ligands and their use as virtual screening filters. *J. Chem. Inf. Comput. Sci.* **2005**, *45*, 160–169. (c) *LigandScout 2.0*; Inte:Ligand GmbH: Vienna, Austria, 2007.

JM070606Z